

VRL3: A DATA-DRIVEN FRAMEWORK FOR VISUAL DEEP REINFORCEMENT LEARNING

Che Wang^{1,2*}

Xufang Luo³

Keith Ross¹

Dongsheng Li³

¹ New York University Shanghai

² New York University

³ Microsoft Research Asia, Shanghai, China

ABSTRACT

We propose a simple but powerful data-driven framework for solving highly challenging visual deep reinforcement learning (DRL) tasks. We analyze a number of major obstacles in taking a data-driven approach, and present a suite of design principles, training strategies, and critical insights about data-driven visual DRL. Our framework has three stages: in stage 1, we leverage non-RL datasets (e.g. ImageNet) to learn task-agnostic visual representations; in stage 2, we use offline RL data (e.g. a limited number of expert demonstrations) to convert the task-agnostic representations into more powerful task-specific representations; in stage 3, we fine-tune the agent with online RL. On a set of highly challenging hand manipulation tasks with sparse reward and realistic visual inputs, our framework learns 370%-1200% faster than the previous SOTA method while using an encoder that is 50 times smaller, fully demonstrating the potential of data-driven deep reinforcement learning.

1 INTRODUCTION

Over the past few years, the sample efficiency of Deep Reinforcement Learning (DRL) has significantly improved in popular benchmarks such as Gym and DMControl. However, the environments in these benchmarks often look very different from the real-world. It remains unclear whether the sample-efficient methodologies developed for these benchmarks can be successfully extended to more practical tasks that rely on realistic visual inputs from cameras and sensors, such as in robotic control and autonomous driving.

A promising direction for DRL is to take a data-driven approach, that is, try to use all the data we can find that might contribute to the learning process. Indeed, in the past few decades, the most important advances in deep learning have been facilitated by the use of large amounts of data and computation (Sutton, 2021; Levine, 2022). Such a data-driven approach is very natural and mature for supervised learning, but not as much so for RL since most DRL methods are designed to work with online data. Although recent advances in representation learning for RL and offline RL reveal the potential of such an approach, there is yet to emerge a data-driven DRL framework that can fully utilize data from multiple different sources and efficiently solve challenging dexterous control tasks from visual inputs.

In this paper, we propose a 3-stage framework designed with such a data-driven mindset. The framework is illustrated in Figure 1. Each stage is designed to utilize a particular type of data source and to address the unique challenges that emerge when these data sources are brought into the DRL process. Here we briefly summarize the core ideas of our framework; a more detailed discussion will follow in later sections.

In stage 1, we learn from large, existing non-RL datasets such as the ImageNet dataset. These datasets might not be directly relevant to the RL task at hand, but they can help us learn task-agnostic visual representations that might be helpful, especially if the RL task also relies on realistic visuals.

*This work was done when Che Wang was interning with Microsoft Research Asia.

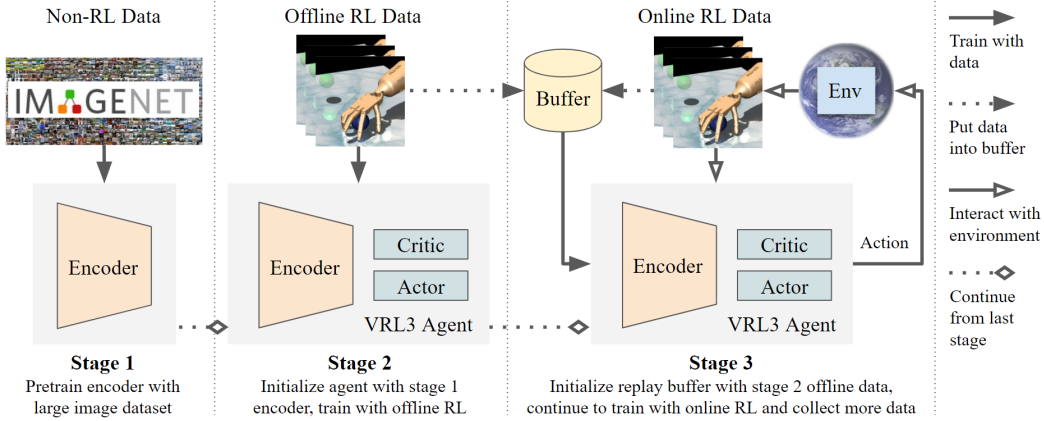


Figure 1: Sample-efficient visual DRL in 3 stages. Following a data-driven approach, in stage 1, we pretrain an encoder using large image datasets, such as ImageNet, in order to obtain a task-agnostic visual representation. In stage 2, we initialize an actor-critic RL agent with the pretrained encoder, and then employ offline RL techniques to exploit offline data to not only train the actor-critic RL agent but also fine-tune the encoder, thereby creating a task-specific encoder. In stage 3, we initialize a buffer with the offline data from stage 2, and further train the agent using online off-policy RL. The idea is very simple: to address highly challenging visual control tasks in the real-world, we want to fully utilize all the available data.

A major challenge here is that the non-RL data can come from a domain that is very different than the RL task, and the input shapes can also be very different. Special care is required to make sure the representations obtained in this stage can be smoothly transferred to the RL task.

In stage 2, we learn from offline RL data, such as a small amount of expert demonstrations, or data collected by a previous learning agent. This offline data is related to the RL task and contains important information about solving the task. We initialize an actor-critic RL agent with the pretrained encoder, and then employ offline RL techniques which not only train the actor-critic RL agent but also fine-tune the encoder, thereby creating a task-specific representations.

In stage 3, we learn from online RL data, which is newly collected data obtained by the actor-critic agent. Our goal is sample efficiency, that is, achieve high performance by collecting as little online data as possible in the third stage. In this stage, we therefore use off-policy training, which uses and re-uses all available data during training. It is important to note that naively applying standard online RL here can lead to severe training instability and completely destroy what we learned from the previous two stages.

Although each stage brings a number of unique challenges, we show that they can be addressed by our framework, allowing us to take full advantage of the different data sources. The key insight of our framework is simple and intuitive: following a data-driven approach and with carefully designed mechanisms to obtain task-specific representations and to stabilize off-policy learning, we are able to efficiently solve highly challenging control tasks with realistic visuals.

Our contributions are as follows:

1. We present Visual Deep Reinforcement Learning in Three Stages (VRL3), a simple and powerful data-driven framework that combines large image datasets, offline RL data, and online RL data to efficiently learn highly challenging tasks with realistic visuals, such as robotic hand manipulation. We carefully analyze the major obstacles in taking this data-driven approach, and show how VRL3 can address these issues. To the best of our knowledge, we are the first to propose a general visual learning framework that can fully utilize all three data sources, and successfully address all the challenges that emerge in such a data-driven approach.
2. We present extensive experimental results and show our proposed method achieves a new level of SOTA sample efficiency on the Adroit hand manipulation suite (from visual input). Compared to the previous SOTA method and averaged over all 4 tasks, VRL3 learns 780%

faster (1200% faster on the most challenging task), reaching an entirely new level of SOTA performance on this very difficult benchmark. We also achieve this strong performance with a tiny encoder that is 50 times smaller. This result clearly demonstrates the great potential of data-driven DRL methods.

3. We present comprehensive experimental analysis and hyperparameter sensitivity study, providing important insights into which of our design decisions are the most critical and which hyperparameters should be tuned with high priority when applied to new tasks. In order to make it easy to use our framework, we will also release pretrained models, data, open source code, and an implementation tutorial.

2 RELATED WORK

The success of VRL3 is built on top of recent advances in representation learning, offline DRL, and online DRL. We now discuss related work, with a focus on related work that uses data from different sources, and how our method is different from prior work. We mainly focus on model-free methods that learn from online data, from demonstrations, and from pretrained representations. Additional related work is discussed in the appendix.

Table 1 summarizes the major differences between VRL3 and some popular visual DRL methods.

Table 1: Comparison among different model-free visual DRL algorithms, VRL3 addresses all the challenges in using non-RL, offline RL and online RL datasets, and can achieve high performance in benchmarks with both simulated and realistic visuals. Note FERM works well in a simpler robotic environment (Zhan et al., 2020), but not in the more challenging Adroit tasks according to results in Shah & Kumar (2021). DMControl tasks are also not tested in the FERM paper; however, FERM is essentially a combination of contrastive methods such as CURL and ATC and data-augmented visual methods such as RAD and DrQ, so it should also work in these benchmarks. For VRL3, note that when we only use stage 3 learning, it essentially becomes a variant of DrQ. DA refers to data augmentation, Con for contrastive learning.

Characteristics	DrQ/RAD	CURL/ATC	FERM	RRL	VRL3
Stage 1	None	None	None	Pretrain	Pretrain
Stage 2	None	None	Con	BC	Offline
Stage 3	DA	Con	DA	No DA	DA
Leverage large visual datasets	×	×	×	✓	✓
Task-specific representations	✓	✓	✓	×	✓
Offline RL data for representations	×	×	✓	×	✓
Offline RL data for policy learning	×	×	×	✓	✓
High data reuse rate (off-policy)	✓	✓	✓	×	✓
Prevent Q network divergence	×	×	×	×	✓
Works in DMC (simulated visuals)	✓	✓	✓	×	✓
Works in Adroit (realistic visuals)	×	×	×	✓	✓

2.1 LEARNING VISUAL TASKS FROM ONLINE RL DATA

Recently, several papers have reported success at learning visual tasks from online visual data. Typically, agents trained with such methods have actor-critic networks, as well as convolutional encoders that extract lower-dimensional features from the visual input. Most of the successful visual online DRL methods are off-policy. A major benefit of using off-policy methods is that they can re-use training data for better sample efficiency.

With the help of data-augmentation, off-policy methods can learn in an end-to-end manner for the easier visual networks (Kostrikov et al., 2020; Yarats et al., 2021a; Laskin et al., 2020a; Yarats et al., 2021b). Within the VRL3 framework, these methods can be seen as only doing stage 3 online RL training, since they do not leverage large existing image datasets, and cannot naively exploit existing offline RL data. Another class of methods use contrastive self-supervised representation learning to solve visual tasks (Laskin et al., 2020b; Stooke et al., 2020; Zhang et al., 2020). Contrastive learning can be used to learn useful representations without gradients from the RL objectives.

These methods work well in simpler environments with simulated visuals, such as in the DMControl environments. However, they can fail entirely if naively applied to highly challenging control tasks with sparse rewards and realistic visuals such as Adroit, due to the difficulty in both exploration and learning representations for realistic visual inputs (Shah & Kumar, 2021). VRL3 also uses off-policy actor-critic methods and data augmentation. But since VRL3 also pretrains with large visual data sets, and further pretrains with offline RL data, it can succeed at the more realistic and challenging Adroit environments.

2.2 LEARNING VISUAL TASKS WITH DEMONSTRATIONS AND REPRESENTATIONS

Zhan et al. (2020) propose FERM, which uses contrastive learning to pretrain an encoder with offline expert demonstrations, and then continues to train online with data augmentation. Under our framework, FERM can be seen as first performing contrastive learning on the encoder in stage 2, and then continuing to train in stage 3 with data augmentation. FERM does not leverage large real-world image datasets, and does not use offline RL techniques to fully exploit offline data in stage 2. FERM can learn simple robotic tasks quickly, but has been shown to be very brittle for the highly challenging Adroit tasks (Shah & Kumar, 2021).

Very recently, RRL (Shah & Kumar, 2021) takes a first step in leveraging ImageNet to obtain task-agnostic representations for visual control tasks. RRL employs a ResNet34 model pretrained on ImageNet and uses it as a fixed feature extractor. Then an on-policy agent is trained with these extracted features. RRL also performs behavioral cloning (BC) on expert demonstrations before starting online learning to overcome exploration issues. Under our framework, RRL can be seen as taking a frozen pretrained encoder in stage 1, using BC updates in stage 2, and then performing *on-policy learning* in stage 3. RRL successfully achieves good performance on Adroit with visual input, including non-trivial performance on the hardest Relocate task.

The major difference between VRL3 and RRL is that we take a more thorough data-driven approach and strive to maximize sample efficiency by exploiting all the available data to the fullest extent. We use a suite of different techniques, including an off-policy backbone and also fine-tuning the encoder to obtain task-specific representations. For computational efficiency, we also use a much smaller encoder rather than large ResNet34 used by RRL. Our experimental results in Section 5 show that VRL3 is 370%-1200% more sample efficient than RRL, depending on the specific Adroit environment (Appendix B), 50 times more parameter efficient in the encoder and 3 times more parameter efficient for all networks in the agent (Appendix C); VRL3 is also more computationally efficient to fully learn the tasks (>90% success), on relocate, VRL3 can solve the task with just 10% of the computation (Appendix D).

2.3 OFFLINE RL AND DATA-DRIVEN RL

In the past few decades, some of the most important advances in research in AI have been based on data-driven methods, so it is natural to ask whether we can also utilize a similar mindset for DRL (Levine, 2022; Sutton, 2021). In this work, we show that our framework can combine the best of the existing works in representation learning, offline RL and online RL, leading to a very simple and powerful data-driven framework.

Off-policy algorithms, typically based on some form of Q-learning, should in principle be able to work with data collected by arbitrary policies. However, they tend to fail entirely when trained in an offline fashion without further interaction with the environment (Fujimoto et al., 2019; Levine et al., 2020). A large number of specialized model-free algorithms have been proposed to tackle these issues and make it possible to fully utilize offline RL data (Fujimoto et al., 2019; Kumar et al., 2020; Chen et al., 2020; Peng et al., 2019; Wu et al., 2019; Kumar et al., 2019; Fujimoto & Gu, 2021; Wang et al., 2018). Under our framework, these methods mainly study how to effectively learn from stage 2 data. There are also a small number of recent works that study the transition from offline to online (Nair et al., 2020; Lee et al., 2022).

Most of the existing work on offline RL focuses on raw-state input and on utilizing existing RL data. In our work we go one step further and show that we can utilize non-RL data as well as RL data to greatly help learning for very challenging tasks that rely on realistic visual inputs.

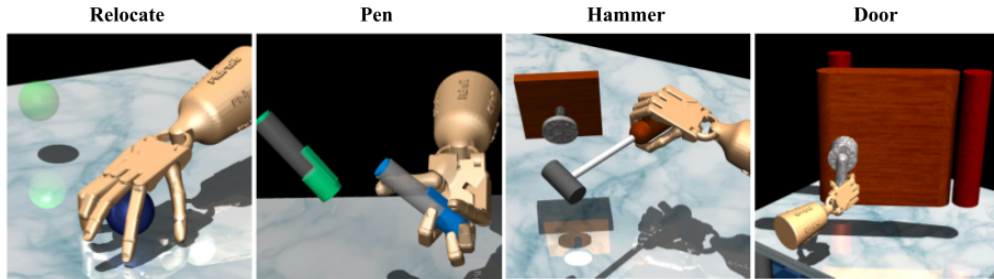


Figure 2: Adroit Suite, figure from Rajeswaran et al. (2017).

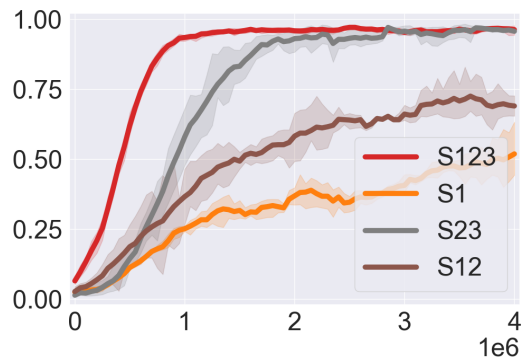
3 MOTIVATIONS, CHALLENGES AND SOLUTIONS IN DATA-DRIVEN VISUAL DRL

We now discuss how our framework is designed. For each stage in our learning framework, we discuss how and why we want to use the data, analyze the major technical challenges, and discuss how we can address these challenges. After fully explaining our design decisions in this section, we will give the exact learning algorithm in the next section.

To better explain the motivations and challenges, we support our arguments with experimental results and findings from the literature. We focus on the Door and Relocate tasks in the Adroit (Figure 2) benchmark. In our figures, X-axis shows number of frames, Y-axis shows success rate in performing the task, unless specified otherwise.

3.1 STAGE 1: PRETRAINING WITH NON-RL DATA

One way to use large non-RL image datasets such as the ImageNet is to pretrain an encoder, and then continue to use this encoder in the downstream RL task, either as a frozen task-agnostic feature extractor (as in RRL) or with task-specific fine-tuning. We advocate combining pretraining with fine-tuning since this gives the best performance, as shown in Figure 3.



(a) Relocate success rate

Figure 3: Effect of training the encoder in each stage. The numbers after “S” indicates the stages where the encoder is trained. S1: pretrain in stage 1 then freeze the encoder. S12: pretrain in stage 1 then fine-tune in stage 2, then freeze. S23: no stage 1 pretrain, finetune in stages 2 and 3. S123(VRL3): pretrain in stage 1, then finetune in stage 2, 3. S123 gives the best performance, showing the benefit to learn both task-agnostic and task-specific representation. A similar observation has been found in transfer learning, where transfer + finetuning gives the best result (Yosinski et al., 2014).

When we pretrain an encoder from large non-RL image datasets such as the ImageNet, the input to the encoder is a single image with RGB channels; for example, a typical ResNet model is trained

with input dimension $3 \times 224 \times 224$. For the downstream RL task, however, it can be beneficial for the agent to take in multiple frames of images as input, so that the agent can learn to use temporal information in consecutive state transitions. And to make computation faster, these frames are typically shrunk to a smaller size such as 84×84 . So the typical input shape for a visual DRL method is $9 \times 84 \times 84$, with 3 frames stacked together, each frame being $3 \times 84 \times 84$.

When we have a stage 1 encoder, how can we modify it so that it works correctly for the downstream RL task in stages 2 and 3? For the mismatch in input channels, one simple solution is to consider each frame as a separate data point, and put them separately into the pretrained encoder, as is done in Shah & Kumar (2021). However, this simple approach has two downsides: 1) it requires more computation, and 2) if we want to further fine-tune the encoder, the encoder cannot learn important temporal and spatial features from the interaction of frames.

Instead, we expand the first convolutional layer of the stage 1 encoder so that it can now take in inputs of 9 channels instead of 3. To achieve this, we repeat the weight matrix three times and then scale all the weight values to $1/3$ of their original values. This allows us to modify the input shape without disrupting the learned representations. Now when we fine-tune the encoder in stages 2 and 3, the encoder can gradually learn to extract useful features from the three frames collectively, without losing information about their temporal and spatial relationship. For the relocate task, we follow Shah & Kumar (2021) and use input from 3 cameras, leading to an input of 27 channels (3 cameras, 3 frames each, with RGB channels); here we repeat the weight 9 times and scale all weight values to $1/9$ th of their original values.

For the mismatch in image shape (84×84 instead of 224×224), note that standard encoders pretrained with 224×224 input can also take in 84×84 input. However, this mismatch can cause a performance drop (Touvron et al., 2019). To avoid this issue, instead of using existing models available in the Internet, we train a new encoder from scratch with images from ImageNet shrunk to 84×84 . To improve computation efficiency and to avoid difficulties in training deep networks in DRL (Bjorck et al., 2021; Ota et al., 2021), we use a light-weight encoder with only 5 convolutional layers, which is 50 times smaller than ResNet34 used in RRL. This allows us to perform experimentation at a much faster pace.

3.2 STAGE 2: OFFLINE RL

With offline RL data, we can fine-tune the task-agnostic representations from stage 1 towards representations that are better suited for the downstream task, and at the same time, we can also learn an offline agent, so that when we switch to online learning in stage 3, we initialize with a partially learned agent instead of a random agent. If the offline RL data consists of expert demonstrations, an on-policy method such as DAPG (Rajeswaran et al., 2017) could simply perform BC in this stage, and then move on to the next stage with the BC policy. However, this has two major drawbacks: 1) the on-policy method cannot use offline RL data other than the expert demonstrations; 2) when moving to online RL in stage 3, on-policy methods discard training data very quickly after updating the policy, leading to low sample efficiency. Aiming for a high sample efficiency, we choose an off-policy method, and now discuss its unique challenges and how to tackle them.

Figure 4 shows that only using BC on expert demonstrations in stage 2 does not give good performance, especially for the Relocate task. This difficulty is due to the distribution shift when transitioning from offline to online, which has been studied in some prior works (Nair et al., 2020).

Special care is required to effectively perform off-policy learning in stage 2. Progress in offline RL research in the past few years show that off-policy methods cannot naively train in an entirely offline manner due to extrapolation errors (Fujimoto et al., 2019; Kumar et al., 2019). In our case, we follow the idea of Conservative Q-Learning (CQL) (Kumar et al., 2020) and add a conservative Q loss term to our standard Q loss; details are discussed in the next section. Figure 5 shows if we naively use off-policy RL updates in stage 2, we run into severe overestimation.

When we fine-tune the encoder in stages 2 and 3, a reduced encoder learning rate can prevent pretrained representations from getting destroyed by noisy RL signals, especially in the early stage of RL training. We find that this helps stabilize training in the Relocate task. This problem has also been observed in other environments (Schwarzer et al., 2021). Figure 6 shows the effect of encoder learning rates.

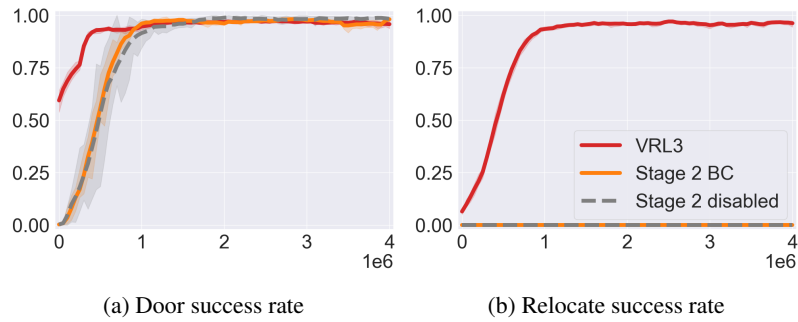


Figure 4: Effect of BC and offline RL updates in stage 2. VRL3 by default uses offline RL updates. Only applying BC or disabling stage 2 training entirely leads to poor performance, especially on Relocate, where their curves overlap at a success rate of zero.

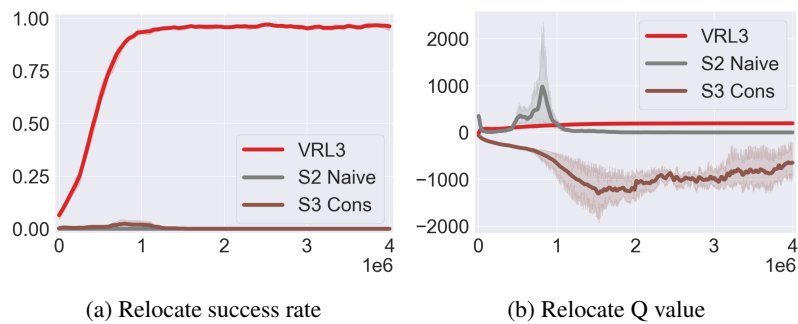


Figure 5: Taking naive RL updates in stage 2 (S2 Naive) leads to an overestimation problem, and taking conservative RL updates in stage 3 (S3 Cons) leads to an underestimation problem.

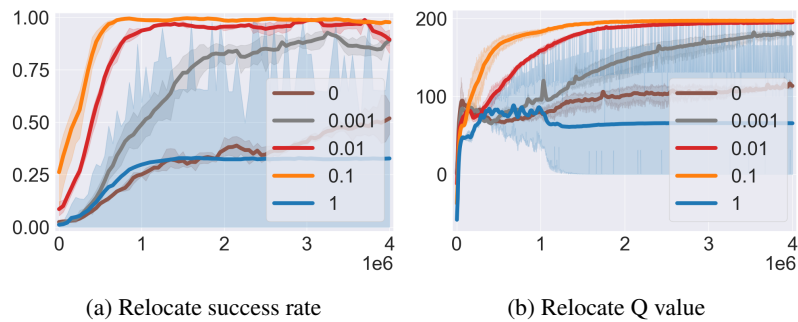


Figure 6: Effect of different encoder learning rates in Relocate (e.g., 0.01 means the encoder’s learning rate is 100 times slower than that for the policy and Q networks.) A frozen encoder causes slow learning, and if encoder learns too fast, it leads to instability.

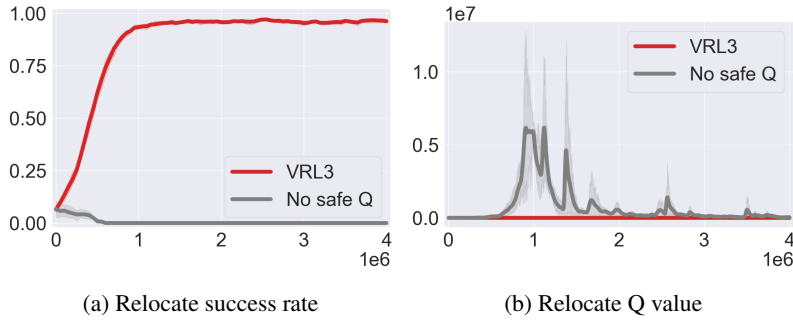


Figure 7: Effect of the safe Q target value technique. Note in our setting, the maximum reasonable Q value should be around 100. When we do not constrain the Q target values, Q estimation bias can quickly accumulate and lead to divergence.

To make our design as simple as possible, and to avoid the entropy collapse problem in SAC (Yarats et al., 2021a), we remove the entropy term in SAC and use a fixed action noise as done in Yarats et al. (2021a). We also use data-augmentation to address the potential problem of overfitting when training with image data. With such a design, we can also further fine-tune the encoder. The encoder is only trained with gradients from the Q loss, following previous methods (Yarats et al., 2021b;a; Laskin et al., 2020a).

In addition to offline RL updates in stage 2, we can still add a number of BC updates before the offline RL updates. As shown in our ablations in the appendix A, BC updates here do not have a visible impact on performance. However, as shown in Rajeswaran et al. (2017), they might still help the agent learn more human-like behaviors.

3.3 STAGE 3: ONLINE RL

Moving from offline to online RL, we again embrace a new set of challenges. First of all, we cannot continue to learn conservative Q values as done in stage 2, because we want the agent to be optimistic instead of pessimistic about new actions and further explore the environment. Nair et al. (2020) show that CQL fails completely when first applied to offline learning and then to online learning. Indeed, Figure 5 shows if we take conservative RL updates in stage 3, we run into severe underestimation.

Even if we remove the conservative terms after entering stage 3, we will still encounter a large inevitable distribution shift caused by the incoming newly collected data, leading to instability, especially in the Q estimates. Indeed, even in standard online training, prior works have shown that a similar problem exists, and is due to a tendency to accumulate (mainly overestimation) bias, a fundamental problem of all Q-learning based methods (Chen et al., 2021; Lan et al., 2020; Fujimoto et al., 2018; Van Hasselt et al., 2016; Thrun & Schwartz, 1993).

A simple and scalable solution is to use an ensemble of Q networks to control the level of bias (Chen et al., 2021). We propose another simple and efficient solution: for all tasks, we set a maximum Q target value. To decide this threshold value, we reshape the maximum per-step reward r_{\max} to be 1, and estimate what the maximum Q value should be for an optimal policy. To be concrete, we can compute the sum of this infinite geometric series, $Q_{\max} = \sum_{t=0}^{\infty} \gamma^t r_{\max} = 100$ when $\gamma = 0.99$. To allow more flexibility in the Q network, we can also set the threshold Q_{\max} to be higher than this value. Now if during any Q update, a Q target value y exceeds this threshold value, then we reduce it to be closer to the threshold value: if $y > Q_{\max} + 1$, then $y \leftarrow Q_{\max} + (y - Q_{\max})^\eta$, where $0 \leq \eta \leq 1$ is the safe Q factor. Notice the $Q_{\max} + 1$ here is a technical detail to address edge cases.

This safe Q target technique allows us to always keep Q values under control and prevent severe problems such as Q divergence. Figure 7 shows that the safe Q target technique is crucial to stable training in stage 3 for the relocate task. Without this constraint on the Q value, training can quickly become unstable and the Q network can entirely diverge.

4 VRL3: VISUAL DRL IN 3 STAGES

In the previous section, we presented a comprehensive discussion on the motivations, the challenges, and our design decisions in taking a 3-stage data-driven approach. We also provided extensive empirical evidence that support our design decisions. After addressing all above mentioned challenges, we now arrive at VRL3. Algorithm 1 gives the pseudocode of VRL3 . We focus on the high-level ideas and provide additional technical details in appendix A.

Algorithm 1 Visual DRL in 3 stages

- 1: Initialize parameterized encoder f_ξ , policy π_ϕ , Q functions $Q_{\theta_1}, Q_{\theta_2}$, Q target functions $Q_{\bar{\theta}_1}, Q_{\bar{\theta}_2}$, empty buffer \mathcal{D} . Set target parameters $\bar{\theta}_i \leftarrow \theta_i$, for $i = 1, 2$. N_{S2} is the number of offline RL updates in stage 2; N_{S3} number of online RL updates for stage 3.
 - 2: Stage 1:
 - 3: Load pretrained encoder parameters into ξ and setup encoder for RL training.
 - 4: Stage 2:
 - 5: Load offline RL data into \mathcal{D}
 - 6: **for** N_{S2} updates **do**
 - 7: Sample a mini-batch B from \mathcal{D}
 - 8: Update f_ξ and $Q_{\theta_1}, Q_{\theta_2}$ with $\mathcal{L}_Q + \mathcal{L}_{QC}$, update π_ϕ with \mathcal{L}_π . Update $Q_{\bar{\theta}_1}, Q_{\bar{\theta}_2}$ with polyak averaging.
 - 9: Stage 3:
 - 10: **for** N_{S3} updates **do**
 - 11: Sample an action from policy, take action and store the new data in \mathcal{D}
 - 12: Sample a mini-batch B from \mathcal{D}
 - 13: Update f_ξ and $Q_{\theta_1}, Q_{\theta_2}$ with \mathcal{L}_Q , update π_ϕ with \mathcal{L}_π . Update $Q_{\bar{\theta}_1}, Q_{\bar{\theta}_2}$ with polyak averaging.
-

Stage 1 We follow the standard supervised learning routine and train a convolutional encoder f_ξ on a 1000-class ImageNet classification task. We follow the standard training procedure of a typical ResNet model. During training we shrink the images to the size of 84x84 so that they match the input dimension of our downstream RL task. In our main results, we also use a light-weight encoder with 5 convolutional layers, with batchnorm after each layer. Since it is shallow, there are no skip connections in this encoder. After we finish stage 1 training, we expand the first convolutional layer of the encoder so the input channel size matches the RL task, as described in the previous section.

Stage 2 We first initialize an RL agent with the pretrained encoder and put the offline RL data in an empty replay buffer \mathcal{D} . For each Adroit task, the offline RL data consists of a total of 25 expert demonstration trajectories. We build our implementation on top of DrQv2 because it is a simple off-policy actor-critic algorithm with superior SOTA performance on DMControl and a very clean and efficient codebase (Yarats et al., 2021a). Here we also try to follow the notations in DrQv2 for better consistency. Our agent has a convolutional encoder, two Q networks, two target Q networks and a policy network.

Let aug denote random shift image augmentation, and cat for concatenation. Let \mathbf{x} be the visual input from the camera (or cameras). In the Adroit environment, in addition to the visual observation, we are also given sensor values from the robotic hand, which is a vector of real numbers, denoted by \mathbf{z} . When using the encoder, we only put the augmented visual input (image frames) into the encoder and obtain a lower-dimensional representation $\mathbf{h} = f_\xi(\text{aug}(\mathbf{x}))$. We then concatenate it with the sensor values. For simplicity, let $\mathbf{s} = \text{cat}(\mathbf{h}, \mathbf{z})$ denote the concatenation; \mathbf{s} is the input to the Q and policy networks, which are multi-layer perceptrons.

For each update, we sample a mini-batch of transitions $(\mathbf{x}_t, \mathbf{z}_t, \mathbf{a}_t, r_{t:t+n-1}, \mathbf{x}_{t+n}, \mathbf{z}_{t+n})$ from the replay buffer \mathcal{D} . Note we have $t+n$ here to compute n-step returns, as done in Yarats et al. (2021a). Let $\mathbf{s}_t = \text{cat}(\mathbf{h}_t, \mathbf{z}_t)$. Let $\tilde{\mathbf{a}}_t \sim \pi_\phi(\mathbf{s}_t)$ be actions sampled from the current policy. The n-step Q target value y is:

$$y = \sum_{i=0}^{n-1} \gamma^i r_{t+i} + \gamma^n \min_{k=1,2} Q_{\bar{\theta}_k}(\mathbf{s}_t, \tilde{\mathbf{a}}_{t+n}). \tag{1}$$

Using the safe Q target value technique discussed in the previous section, if $y > Q_{\max} + 1$, then we modify y to a ‘‘safer’’ value: $y \leftarrow Q_{\max} + (y - Q_{\max})^\eta$.

The standard Q loss \mathcal{L}_Q is (for $k = 1, 2$):

$$\mathcal{L}_Q(\mathcal{D}) = \mathbb{E}_{\tau \sim \mathcal{D}} [(Q_{\theta_k}(\mathbf{h}_t, \mathbf{a}_t) - y)^2], \quad (2)$$

Following Kumar et al. (2020), and build on top of our framework, the additional conservative Q loss \mathcal{L}_{QC} is:

$$\mathcal{L}_{QC}(\mathcal{D}) = \mathbb{E}_{\tau \sim \mathcal{D}} [\log \sum_{\tilde{\mathbf{a}}_t} \exp(Q(\mathbf{s}_t, \tilde{\mathbf{a}}_t)) - Q(\mathbf{s}_t, \mathbf{a}_t)], \quad (3)$$

On a high-level, this loss essentially reduces the Q value for actions proposed by the current policy, and increase the Q values for actions in the replay buffer (Kumar et al., 2020). Additional technical details can be found in appendix A.

The policy (actor) loss \mathcal{L}_π is:

$$\mathcal{L}_\phi(\mathcal{D}) = -\mathbb{E}_{\tau \sim \mathcal{D}} [\min_{k=1,2} Q_{\theta_k}(\mathbf{s}_t, \mathbf{a}_t)]. \quad (4)$$

Let α be the learning rate for the policy network and the Q networks. Let β_{enc} be the encoder learning rate scale, so that the encoder learning rate is $\alpha_{\text{enc}} = \beta_{\text{enc}}\alpha$. For each offline RL update in stage 2, we perform gradient descent on $\mathcal{L}_Q(\mathcal{D}) + \mathcal{L}_{QC}(\mathcal{D})$ to update the encoder f_ξ and the Q networks $Q_{\theta_1}, Q_{\theta_2}$, and gradient descent on \mathcal{L}_π to update the policy π_ϕ . Note that we do not use the gradient from the policy to update the encoder, following previous work (Yarats et al., 2021b;a).

$$\xi \leftarrow \xi - \alpha_{\text{enc}} \nabla_\xi (\mathcal{L}_Q(\mathcal{D}) + \mathcal{L}_{QC}(\mathcal{D})) \quad (5)$$

$$\theta_k \leftarrow \theta_k - \alpha \nabla_{\theta_k} (\mathcal{L}_Q(\mathcal{D}) + \mathcal{L}_{QC}(\mathcal{D})) \quad k \in \{1, 2\} \quad (6)$$

$$\phi \leftarrow \phi - \alpha \nabla_\phi \mathcal{L}_\pi(\mathcal{D}) \quad (7)$$

The Q target networks $Q_{\bar{\theta}_1}$ and $Q_{\bar{\theta}_2}$ are updated with polyak averaging.

$$\bar{\theta}_k \leftarrow (1 - \tau)\bar{\theta}_k + \tau\theta_k \quad k \in \{1, 2\} \quad (8)$$

Stage 3 We continue to use the replay buffer \mathcal{D} , which already contains the offline RL data. We now perform standard online RL, and newly collected data are added to \mathcal{D} .

The update is the same as in stage 2, except we remove the conservative Q loss \mathcal{L}_{QC} :

$$\xi \leftarrow \xi - \alpha_{\text{enc}} \nabla_\xi \mathcal{L}_Q(\mathcal{D}) \quad (9)$$

$$\theta_k \leftarrow \theta_k - \alpha \nabla_{\theta_k} \mathcal{L}_Q(\mathcal{D}) \quad \forall k \in \{1, 2\} \quad (10)$$

$$\phi \leftarrow \phi - \alpha \nabla_\phi \mathcal{L}_\pi(\mathcal{D}) \quad (11)$$

The Q target networks $Q_{\bar{\theta}_1}$ and $Q_{\bar{\theta}_2}$ are again updated with polyak averaging.

$$\bar{\theta}_k \leftarrow (1 - \tau)\bar{\theta}_k + \tau\theta_k \quad k \in \{1, 2\} \quad (12)$$

5 RESULTS

We focus on performance comparison between VRL3 and RRL, the previous SOTA on Adroit. RRL is also the only method that achieves non-trivial performance on the most challenging relocate task with visual input. We also compare with DrQv2 and FERM. Note that DrQv2 does not naively learn in Adroit due to the difficulty in exploration, and FERM has brittle performance on Adroit Shah & Kumar (2021). To create stronger baselines, we introduce DrQv2(VRL3), a variant of DrQv2 which starts stage 3 training with demonstrations in the buffer, similar to Vecerik et al. (2017), and is built on top of our framework. We also introduce FERM(VRL3), a variant of FERM built on top of our framework, which uses contrastive learning in stage 2 and fine-tuning in stage 3 with data augmentation. By doing so we greatly improve the performance of both baselines, making our comparison more fair. Figure 8 shows performance comparison on all 4 Adroit tasks. Compared to the fine-tuned FERM results in Shah & Kumar (2021), our FERM(VRL3) has much stronger and more robust performance. Interestingly, both FERM(VRL3) and DrQv2fD(VRL3) outperform RRL in Door, Hammer and Pen, showing that on easier tasks, these off-policy agents can learn very fast even without stage 1 representations. On the more difficult Relocate task, however, both fail to learn anything, showing the importance of stage 1 representation in the most challenging tasks. VRL3 has the best performance and outperforms RRL by a significant margin in all 4 environments, reaching a new level of SOTA performance on this benchmark.

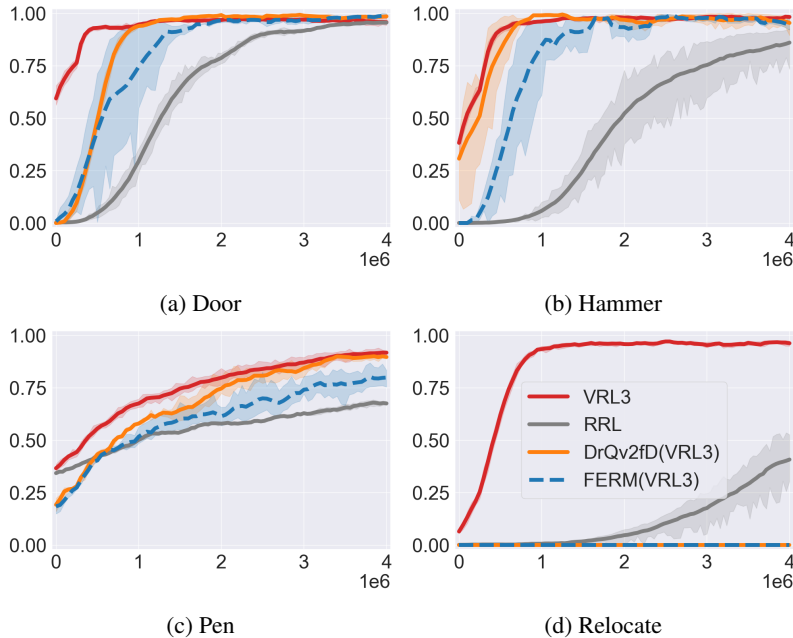


Figure 8: Performance comparison of VRL3, RRL (the previous SOTA), DrQv2fD(VRL3), FERM(VRL3) on 4 visual Adroit tasks. The performance for VRL3 is averaged over 10 seeds (seeds 0-9). To ensure consistency with prior work, results for RRL are from log files provided by the authors. VRL3(FERM) is our implementation of FERM which performs much stronger than the results in Shah & Kumar (2021) and DrQv2fD(VRL3) is a DrQv2 variant that take advantage of demonstrations. However, both cannot learn relocate due to lack of stage 1 representations and insufficient exploitation of stage 2 data. Prior to our work, RRL was the best performing method on this benchmark, and it was the only method that achieved non-trivial performance on Relocate.

5.1 ADDITIONAL STUDIES AND ANALYSIS

In appendix A, we present a comprehensive study on hyperparameter robustness and sensitivity, which provide additional insights. In addition to the important design decisions discussed in section 3, we found that the learning rate, the encoder learning rate scale, and the action exploration noise (std for action distribution) are three very important hyperparameters that can have a large impact on performance. When VRL3 is applied to a new task, these hyperparameters should be tuned with high priority.

6 DISCUSSION AND FUTURE WORK

In this paper, we proposed a simple and powerful 3-stage data-driven framework for effective DRL for realistic visual control tasks. We carefully analyzed the challenges in taking a data-driven approach and showed how our framework can address these challenges, allowing us to greatly benefit from different sources of data. All our design decisions are supported by experiment results, ablation studies and findings in the literature. Our methodology achieves a new SOTA sample efficiency on the difficult Adroit benchmark, outperforming the previous SOTA by a very significant 370%-1200%. We additionally provided a comprehensive hyperparameter robustness analysis and useful recommendations on applying our framework to other tasks. We believe our work takes an important step towards practical data-driven DRL for highly challenging real world tasks that rely on visual input and opens up a number of exciting future research directions in data-driven deep reinforcement learning.

REFERENCES

- Johan Bjorck, Carla P Gomes, and Kilian Q Weinberger. Towards deeper deep reinforcement learning. *arXiv preprint arXiv:2106.01151*, 2021.
- Xinyue Chen, Zijian Zhou, Zheng Wang, Che Wang, Yanqiu Wu, and Keith Ross. Bail: Best-action imitation learning for batch deep reinforcement learning. In *Advances in Neural Information Processing Systems*, volume 33, pp. 18353–18363, 2020.
- Xinyue Chen, Che Wang, Zijian Zhou, and Keith Ross. Randomized ensembled double q-learning: Learning fast without a model. *International Conference on Learning Representations*, 2021.
- Karl W Cobbe, Jacob Hilton, Oleg Klimov, and John Schulman. Phasic policy gradient. In *International Conference on Machine Learning*, pp. 2020–2027. PMLR, 2021.
- Yan Duan, Xi Chen, Rein Houthoofd, John Schulman, and Pieter Abbeel. Benchmarking deep reinforcement learning for continuous control. In *International Conference on Machine Learning*, pp. 1329–1338, 2016.
- Scott Fujimoto and Shixiang Shane Gu. A minimalist approach to offline reinforcement learning. *arXiv preprint arXiv:2106.06860*, 2021.
- Scott Fujimoto, Herke van Hoof, and Dave Meger. Addressing function approximation error in actor-critic methods. *arXiv preprint arXiv:1802.09477*, 2018.
- Scott Fujimoto, David Meger, and Doina Precup. Off-policy deep reinforcement learning without exploration. In *International Conference on Machine Learning*, pp. 2052–2062. PMLR, 2019.
- Peter Henderson, Riashat Islam, Philip Bachman, Joelle Pineau, Doina Precup, and David Meger. Deep reinforcement learning that matters. In *Thirty-Second AAAI Conference on Artificial Intelligence*, 2018.
- Riashat Islam, Peter Henderson, Maziar Gomrokchi, and Doina Precup. Reproducibility of benchmarked deep reinforcement learning tasks for continuous control. *arXiv preprint arXiv:1708.04133*, 2017.
- Ilya Kostrikov, Denis Yarats, and Rob Fergus. Image augmentation is all you need: Regularizing deep reinforcement learning from pixels. *arXiv preprint arXiv:2004.13649*, 2020.
- Aviral Kumar, Justin Fu, George Tucker, and Sergey Levine. Stabilizing off-policy q-learning via bootstrapping error reduction. *arXiv preprint arXiv:1906.00949*, 2019.
- Aviral Kumar, Aurick Zhou, George Tucker, and Sergey Levine. Conservative q-learning for offline reinforcement learning. *arXiv preprint arXiv:2006.04779*, 2020.
- Qingfeng Lan, Yangchen Pan, Alona Fyshe, and Martha White. Maxmin q-learning: Controlling the estimation bias of q-learning. *arXiv preprint arXiv:2002.06487*, 2020.
- Michael Laskin, Kimin Lee, Adam Stooke, Lerrel Pinto, Pieter Abbeel, and Aravind Srinivas. Reinforcement learning with augmented data. *arXiv preprint arXiv:2004.14990*, 2020a.
- Michael Laskin, Aravind Srinivas, and Pieter Abbeel. Curl: Contrastive unsupervised representations for reinforcement learning. In *International Conference on Machine Learning*, pp. 5639–5650. PMLR, 2020b.
- Seunghyun Lee, Younggyo Seo, Kimin Lee, Pieter Abbeel, and Jinwoo Shin. Offline-to-online reinforcement learning via balanced replay and pessimistic q-ensemble. In *Conference on Robot Learning*, pp. 1702–1712. PMLR, 2022.
- Sergey Levine. Understanding the world through action. In *Conference on Robot Learning*, pp. 1752–1757. PMLR, 2022.
- Sergey Levine, Aviral Kumar, George Tucker, and Justin Fu. Offline reinforcement learning: Tutorial, review, and perspectives on open problems. *arXiv preprint arXiv:2005.01643*, 2020.

- Ashvin Nair, Murtaza Dalal, Abhishek Gupta, and Sergey Levine. Awac: Accelerating online reinforcement learning with offline datasets. 2020.
- Kei Ota, Devesh K Jha, and Asako Kanezaki. Training larger networks for deep reinforcement learning. *arXiv preprint arXiv:2102.07920*, 2021.
- Xue Bin Peng, Aviral Kumar, Grace Zhang, and Sergey Levine. Advantage-weighted regression: Simple and scalable off-policy reinforcement learning. *arXiv preprint arXiv:1910.00177*, 2019.
- Aravind Rajeswaran, Vikash Kumar, Abhishek Gupta, Giulia Vezzani, John Schulman, Emanuel Todorov, and Sergey Levine. Learning complex dexterous manipulation with deep reinforcement learning and demonstrations. *arXiv preprint arXiv:1709.10087*, 2017.
- Max Schwarzer, Nitarshan Rajkumar, Michael Noukhovitch, Ankesh Anand, Laurent Charlin, Devon Hjelm, Philip Bachman, and Aaron Courville. Pretraining representations for data-efficient reinforcement learning. *arXiv preprint arXiv:2106.04799*, 2021.
- Rutav Shah and Vikash Kumar. Rrl: Resnet as representation for reinforcement learning. In *Self-Supervision for Reinforcement Learning Workshop-ICLR 2021*, 2021.
- Adam Stooke, Kimin Lee, Pieter Abbeel, and Michael Laskin. Decoupling representation learning from reinforcement learning. *arXiv preprint arXiv:2009.08319*, 2020.
- Richard S Sutton. The bitter lesson. <http://www.incompleteideas.net/IncIdeas/BitterLesson.html>, 2021. Accessed: 2022-01-24.
- Yuval Tassa, Yotam Doron, Alistair Muldal, Tom Erez, Yazhe Li, Diego de Las Casas, David Budden, Abbas Abdolmaleki, Josh Merel, Andrew Lefrancq, et al. Deepmind control suite. *arXiv preprint arXiv:1801.00690*, 2018.
- Sebastian Thrun and Anton Schwartz. Issues in using function approximation for reinforcement learning. In *Proceedings of the 1993 Connectionist Models Summer School Hillsdale, NJ. Lawrence Erlbaum*, 1993.
- Hugo Touvron, Andrea Vedaldi, Matthijs Douze, and Hervé Jégou. Fixing the train-test resolution discrepancy. *arXiv preprint arXiv:1906.06423*, 2019.
- Hado Van Hasselt, Arthur Guez, and David Silver. Deep reinforcement learning with double q-learning. In *AAAI*, volume 2, pp. 5. Phoenix, AZ, 2016.
- Mel Vecerik, Todd Hester, Jonathan Scholz, Fumin Wang, Olivier Pietquin, Bilal Piot, Nicolas Heess, Thomas Rothörl, Thomas Lampe, and Martin Riedmiller. Leveraging demonstrations for deep reinforcement learning on robotics problems with sparse rewards. *arXiv preprint arXiv:1707.08817*, 2017.
- Qing Wang, Jiechao Xiong, Lei Han, Han Liu, Tong Zhang, et al. Exponentially weighted imitation learning for batched historical data. In *Advances in Neural Information Processing Systems*, pp. 6288–6297, 2018.
- Yifan Wu, George Tucker, and Ofir Nachum. Behavior regularized offline reinforcement learning. *arXiv preprint arXiv:1911.11361*, 2019.
- Mengjiao Yang and Ofir Nachum. Representation matters: Offline pretraining for sequential decision making. *arXiv preprint arXiv:2102.05815*, 2021.
- Denis Yarats, Rob Fergus, Alessandro Lazaric, and Lerrel Pinto. Mastering visual continuous control: Improved data-augmented reinforcement learning. *arXiv preprint arXiv:2107.09645*, 2021a.
- Denis Yarats, Ilya Kostrikov, and Rob Fergus. Image augmentation is all you need: Regularizing deep reinforcement learning from pixels. In *International Conference on Learning Representations*, 2021b. URL <https://openreview.net/forum?id=GY6-6sTvGaf>.
- Jason Yosinski, Jeff Clune, Yoshua Bengio, and Hod Lipson. How transferable are features in deep neural networks? *arXiv preprint arXiv:1411.1792*, 2014.

Albert Zhan, Philip Zhao, Lerrel Pinto, Pieter Abbeel, and Michael Laskin. A framework for efficient robotic manipulation. *arXiv preprint arXiv:2012.07975*, 2020.

Amy Zhang, Rowan McAllister, Roberto Calandra, Yarín Gal, and Sergey Levine. Learning invariant representations for reinforcement learning without reconstruction. *arXiv preprint arXiv:2006.10742*, 2020.

A HYPERPARAMETER ROBUSTNESS, SENSITIVITY AND UNDERSTANDING

In this section we discuss implementation details and present an extensive ablation study on hyperparameters.

Figure 9 shows how each hyperparameter affect training performance. For each figure, the results show how learning is affected when we modify one hyperparameter from our set of default hyperparameters while keeping all the rest fixed as the default values. Following our 3-stage framework, we discuss hyperparameters that affect one or more stages of our training process, and we also give our default value for each hyperparameter. The default hyperparameters are found in our early experiments with random search.

The goal here is to achieve a thorough understanding of what components are the most important for VRL3 to work, and when VRL3 is applied to a new task, which ones of the hyperparameters are the most critical and should be finetuned first. We believe these insights can greatly help researchers and practitioners in applying our framework to new visual tasks, or build research on top of our work.

A.1 STAGE 1

Stage 1: whether we use stage 1 pretraining (default: True). If we perform stage 1 pretraining, then we start with an encoder that is pretrained on the ImageNet dataset, otherwise we start with a random encoder. This will only affect the initialization of encoder for stage 2 and 3. Figure 9a shows that the door task actually does not rely on stage 1 features, but the more challenging relocate task benefit hugely from stage 1 pretraining. This observation is consistent with previous results that show more difficult tasks benefit more from pretrained features, and easier tasks can be learned without them (Shah & Kumar, 2021). This result shows that stage 1 pretraining is critical especially if we want to tackle highly challenging real-world control tasks.

A.2 HYPERPARAMETERS THAT AFFECT BOTH STAGE 2 AND 3

During our training in stage 2 and stage 3, we can also add an additional BC loss, which can help the agent learn more human-like behavior (Rajeswaran et al., 2017). We do not include it in Algorithm 1 since it does not have a significant impact on performance, but will discuss it in this ablation study.

Stage 2 and 3: whether we use data augmentation (default: True). Figure 9b shows that data augmentation is critical for both tasks. This result is consistent with previous literature that found data augmentation such as random shift can greatly improve performance in visual-based tasks (Yarats et al., 2021a;b). Although previous works mainly apply data augmentation to tasks with visuals that are very different from the real-world such as DMControl(Tassa et al., 2018), we show that it can also improves performance in tasks with realistic visuals.

Stage 2 and 3: demonstration replay batch size (default: 64). In stage 2, before the offline RL updates, we perform a number of BC updates where we sample from a demonstration replay buffer. In stage 3, we also do BC with a decaying loss. Figure 9g shows that the batch size for computing BC loss is not very important. By default, we use a small batch size of 64 to reduce computation time.

Stage 2 and 3: encoder learning rate scale (default: 0.01 for relocate, and 1 for the other tasks). Figure 9c shows that when encoder is fixed (learning rate scale is 0), then the performance becomes worse, especially for relocate. Note that when encoder learning rate is too high, learning can also become difficult. For relocate, we reduce its encoder learning rate to be 100 times slower than the learning rate for other parts of the agent, similar to what is done in Schwarzer et al. (2021). This result, together with Figure 9a shows that when task-agnostic representation is finetuned towards task-specific representation learned directly from RL objective with data augmentation gives the best performance.

Stage 2 and 3: learning rate (default: $1e - 4$). Figure 9d shows that (unsurprisingly), when learning rate becomes too small or too large, performance will drop.

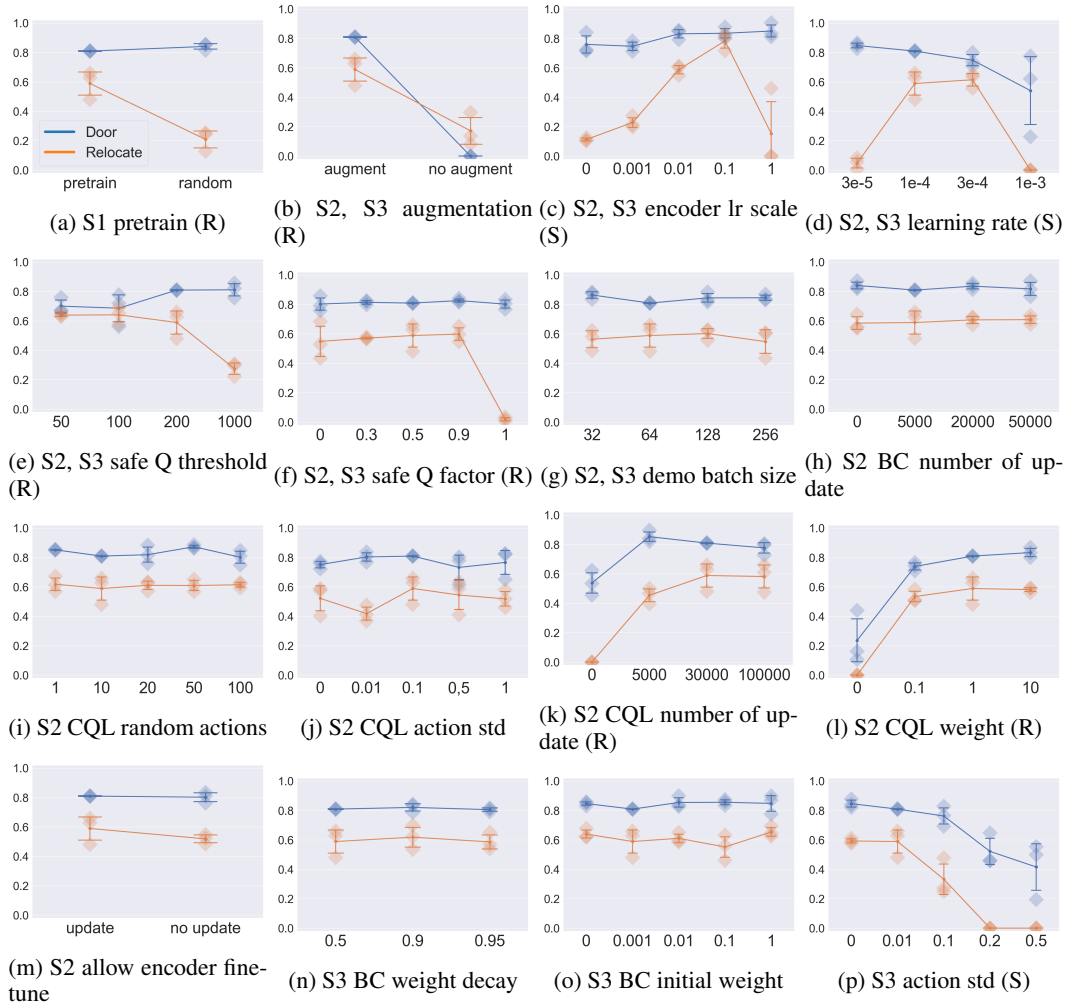


Figure 9: Hyperparameter sensitivity study for all three stages, blue shows the door task, orange shows the more difficult relocate task. For each figure, caption shows the type of hyperparameter, X-axis shows different hyperparameter values, Y-axis shows the average success rate in the first 1M frames of training, averaged over three seeds. Each dot is the average success rate of one seed, error bar shows one standard deviation. We use (S) to denote critical hyperparameter that is relatively sensitive and should be tuned with high priority when applied to a new task. (R) denotes critical hyperparameter that is robust or very easy to tune. Hyperparameters that are mentioned in the main paper are discussed in the appendix.

Stage 2 and 3, safe Q target value threshold (default: 200): Figure 9e shows that having a reasonable Q value threshold greatly helps improve performance on relocate. As described in the main text, This threshold decides how large the Q value can become. Having this safe Q target value technique allows easy control excessive Q bias accumulation with minimal negative effect.

Stage 2 and 3, safe Q factor (default: 0.5): Figure 9f shows that having a safe Q factor that is < 1 (when it is 1, then we are not limiting how large the Q values can be) can help stabilize training and prevent performance issues caused by Q divergence.

A.3 STAGE 2 HYPERPARAMETERS

In stage 2, most of the hyperparameters here are about the offline updates. As mentioned in the previous section, we can have optional BC updates before the offline RL updates. For the offline RL updates, since we mainly use the idea of CQL, there are a number of CQL relevant hyperparameters.

Stage 2, number of BC update (default: 5000): Figure 9h shows that BC updates in stage 2 before taking offline RL updates in fact does not affect performance too much. In terms of performance, it might not be necessary when offline RL is applied at stage 2. However, it can still help the agent learn more human-like behaviors, as discussed in Rajeswaran et al. (2017).

Stage 2, CQL number of random actions (default: 10): in the author’s implementation of CQL, a number of random actions are generated from a uniform distribution and these actions are used in the log-sum-exp computation along with actions proposed by the current policy. Though this is not really discussed in the CQL paper (Kumar et al., 2020), the number of random actions might have an effect on offline training. Figure 9i shows that in our case, the number of random actions for CQL updates in stage 2 does not have a significant effect. However, we recommend future researchers to test this hyperparameter when applying VRL3 to new tasks, since the effect of this small detail is not fully addressed by the CQL authors.

Stage 2, CQL action std (default: 0.1): since our off-policy backbone is DrQv2, we no longer have the entropy term in SAC, but use a fixed action std during updates and during exploration. We also test the effect of this std in stage 2 offline RL updates. Figure 9j shows that in our case, the standard deviation for the action distribution during CQL updates do not have a significant effect on training. Note that however, as we will discuss in the next subsection, this action std has a significant effect in stage 3 online learning.

Stage 2, CQL number of updates (default: 30000): Figure 9k shows that when we do not use offline RL updates (0 updates), then BC updates in stage 2 alone cannot guarantee good performance in stage 3. Some of this difficulty has been studied in Nair et al. (2020).

Stage 2, CQL weight (default: 1): this weight decides how hard the Q values are being affected by the conservative loss term (Kumar et al., 2020). Figure 9l shows that when CQL weight is greater than 0, the performance is in general robust with different values.

Stage 2, allow encoder finetune in stage 2 (default: True): by default, in stage 2 we finetune encoder with Q loss. Does this stage 2 finetuning have a significant effect on performance? Figure 9m shows that this does not affect performance too much in our case, indicating that for the encoder, stage 1 pretraining plus stage 3 finetuning is enough to obtain good performance. This shows in stage 2 we can do more than just using stage 2 data to learn representations. We can get the best performance by fully exploiting stage 2 data to learn an offline RL agent as well as improved representations,

A.4 STAGE 3 HYPERPARAMETERS

Stage 3, BC weight decay (default: 0.5): this value decides how fast the BC loss is decayed, following (Rajeswaran et al., 2017). Figure 9n shows that under our current design of VRL3, the decaying speed of BC loss does not affect performance too much.

Stage 3, BC initial weight (default: 0.001): The initial weight of the BC loss. Figure 9o shows that initial BC weight in stage 3 does not have a significant effect on performance. Again, we keep the BC loss here since it can also help the robotic hand learn human-like behaviors.

Stage 3, action distribution standard deviation for exploration (default: 0.01): Figure 9p shows that we need a small std value to obtain good performance. This is likely because the Adroit tasks have sparse reward, thus it is easier to have less action noise so that the agent focus on exploring state space that is close to the expert demonstrations. This is another very important hyperparameter that will require tuning on a new task. Note that in some other benchmarks such as DMControl, the exploration action noise is typically much larger.

B SAMPLE EFFICIENCY COMPARISON

Table 2 shows a comparison of VRL3 and RRL in terms of sample efficiency. Sample efficiency is important because online data can be hard and expensive to obtain in DRL control tasks. Being able to reach a high sample efficiency means we can solve the task faster and with much less cost. Results show that VRL3 has much better sample efficiency in all tasks, giving an average of 780% times better sample efficiency in reaching 90% success rate in all Adroit tasks, with a very impressive 1200% better sample efficiency on the most challenging relocate task.

Table 2: Sample efficiency comparison of VRL3 and RRL. The numbers show the number of data (frames) collected when the specified success rate is achieved. (to be precise, the frame number indicates the agent has an average success rate that is equal or greater than the specified success rate for the past 20K frames of training.) The last column show how many times VRL3 is more sample efficient than RRL in reaching that success rate. VRL3 is very efficient in learning especially when aiming for a high success rate. Averaged over all Adroit tasks, we are 7.8 times more sample efficient than RRL, the previous SOTA method, to reach 90% success rate. To ensure our performance is not the result of “lucky random seeds”(Henderson et al., 2018; Islam et al., 2017; Duan et al., 2016), the performance for VRL3 is averaged over 10 seeds. To ensure consistency with prior work, results for RRL are directly from the training log files provided by the authors. Note in the pen task, RRL’s success rate at 12M is slightly less than 90%, but very close.

Score	RRL	VRL3	VRL3 faster
Door at 50%	1360K	200K	6.8
Door at 75%	1880K	300K	6.3
Door at 90%	2560K	400K	6.4
Hammer at 50%	2080K	250K	8.3
Hammer at 75%	3120K	350K	8.9
Hammer at 90%	4440K	500K	8.9
Pen at 50%	1120K	400K	2.8
Pen at 75%	6200K	1600K	3.9
Pen at 90%	12000K	3250K	3.7
Relocate at 50%	4360K	500K	8.7
Relocate at 75%	6800K	650K	10.5
Relocate at 90%	11000K	900K	12.2

C PARAMETER EFFICIENCY COMPARISON

Table 3 gives a comparison of number of parameters for VRL3 and RRL. Note that in addition to the encoder, other networks in the agent can also have a lot of parameters, so we have to approach this comparison carefully. Note that VRL3 has a much smaller encoder and relatively larger MLP critic and actor networks. If we count all the parameters in the agent, then VRL3 has about 37% of the parameters as used in RRL with a ResNet34. Note that being parameter-efficient is also not exactly the same as being computationally efficient. In the next section, we discuss computation efficiency.

Table 3: Parameter efficiency comparison of RRL and VRL3. We compare the number of parameters in the encoder part, as well as parameters for all networks in the agent. Note that VRL3 has a much smaller encoder, but relatively larger critic and policy (actor) networks, VRL3 also has a pair of critic networks instead of just one. For encoder, VRL3 is more than 50 times more parameter efficient. Overall, VRL3 is about 3 times more parameter efficient.

Number of parameters (M)	RRL	VRL3	VRL3/RRL ratio
Encoder	21.28	0.40	0.0187
Policy network	2.0	3.0	1.5
Critic networks	2.0	6.0	3
All	25.28	9.4	0.37

D COMPUTATION EFFICIENCY COMPARISON

We now compare the computation efficiency of RRL and VRL3 . We do not take into account the time used for agent evaluation (in which case RRL is much slower due to the large ResNet34 encoder) for RRL we use the authors' codebase. On a single NVIDIA V100 GPU, for door, RRL runs at 83 FPS while VRL3 runs at 68 FPS; for relocate, RRL runs at 53 FPS while VRL3 runs at 47 FPS.

Note that RRL is faster in per-frame computation mainly because its encoder is frozen, so images only need to be processed by the encoder once when they are collected. For VRL3, although the encoder is 50 times smaller, the encoder will be updated in all stages, and the off-policy method we are based on also use a larger batch size and larger actor and critic networks. Note that although VRL3 will take a bit longer time to train for the same number of frames, it is significantly faster when we consider the fact that it can learn a task with a very small amount of online data. In terms of the computation time used to reach 90% success rate, VRL3 is much faster on all tasks, and more than 10 times faster on the most challenging relocate task. Note that here we are not considering acceleration from parallel or multi-core computing.

Table 4: Computation efficiency comparison of RRL and VRL3.

Computation Time (Hours)	RRL	VRL3	VRL3/RRL ratio
Door, Pen, Hammer (4M)	13.39	16.34	1.22
Relocate (4M)	20.96	23.64	1.13
Door (90% success)	8.57	1.63	0.19
Hammer (90% success)	14.86	2.04	0.14
Pen (90% success)	40.16	13.28	0.33
Relocate (90% success)	57.65	5.32	0.09

E COMPUTING INFRASTRUCTURE

Our experiments are conducted on NVIDIA Tesla P40, P100 and V100 GPUs. When calculating the computation efficiency table, we use a single V100 GPU.

F DISCUSSION ON FUTURE WORK

The success of VRL3 opens up a number of exciting future research directions in data-driven DRL.

One direction is to use on-policy methods in the VRL3 framework. Although on-policy methods tend to have worse sample efficiency due to the difficulty of using off-policy data, recent studies show that on-policy methods can use data many more times to learn useful features with value distillation (Cobbe et al., 2021). In this way it might possible to combine the unique advantages of on-policy methods with the effectiveness of a data-driven approach.

Model-based methods can be used together with VRL3. Model-based methods tend to be more complex than model-free ones, however, these models are typically learned in a supervised manner, making them good candidates for building advanced data-driven methods.

Contrastive pretraining techniques can also be very useful in such a data-driven approach. Although our experiments show that contrastive representation learning in stage 2 alone do not work well, they can be combined with data-augmented offline and online RL. Recently, a number of methods have shown that model-based and contrastive methods can help accelerate online learning (Schwarzer et al., 2021; Yang & Nachum, 2021). In our current design, for stage 2 and 3, we use data coming from the exact RL task we want to solve. It is also possible to utilize data from RL tasks that are related, but are not exactly the task we are solving. Here contrastive pretraining has a lot of potential.

Another important direction is to understand how the domain difference between data sources affect the learning process and how we can best utilize stage 1 data when the RL task environment has very different visuals.